THE ASTROPHYSICAL JOURNAL, 386:L13–L16, 1992 February 10


# POSSIBLE MODELS FOR THE TYPE Ia SUPERNOVA 1990N

TOSHIKAZU SHIGEYAMA
Max-Planck-Institut für Astrophysik, D8046 Garching bei München, Germany
KEN'ICHI NOMOTO AND HITOSHI YAMAOKA
Department of Astronomy, Faculty of Science, University of Tokyo, Tokyo 113, Japan
AND
FRIEDRICH-KARL THIELEMANN
Harvard-Smithsonian Center for Astrophysics, Cambridge, MA 02138
*Received 1991 August 20; accepted 1991 November 26*

## ABSTRACT

Possible interpretations of new spectral and photometric features of Type Ia supernova 1990N with carbon deflagration/detonation models are presented. To explain the presence of Si and Ca at high expansion velocities in SN 1990N, we suggest four possible models, among which is a carbon detonation in a white dwarf with a mass $\sim 1\ M_\odot$. The slow rise of the light curve of SN 1990N can be reproduced by both the deflagration and detonation models if the optical opacity is somewhat larger than that previously adopted. Implications for the Hubble constant are discussed.

*Subject headings:* galaxies: distances and redshifts — nuclear reactions, nucleosynthesis, abundances — stars: individual (SN 1990N) — supernovae: individual (SN 1990N) — white dwarfs

## 1. INTRODUCTION

Type Ia supernovae (SNe Ia) are characterized by the absence of hydrogen and the presence of P-Cygni profiles of Fe, Ca, S, Si, Mg, and O in the spectrum near maximum light. Later the spectral features and the light curve shapes of SNe Ia have been well modeled by the carbon deflagration of accreting white dwarfs (Nomoto, Sugimoto, & Neo 1976; Nomoto, Thielemann, & Yokoi 1984; Branch et al. 1985; Woosley & Weaver 1986b). The good agreement between the calculated and observed spectra (especially near maximum light; Branch et al. 1985; Harkness 1991) implies that the composition structure as a function of expansion velocity $v_{\rm exp}$ of SNe Ia must be similar to the carbon deflagration model W7, which is characterized by the presence of Ca and Si at $v_{\rm exp} \gtrsim 8000$ km s$^{-1}$ (Nomoto et al. 1984). Note, however, the serious remaining uncertainties associated with the presupernova evolution of binary systems, the initiation of a deflagration/detonation, and the propagation of the burning front (see Wheeler & Harkness 1990 for a review).

Recently SN Ia 1990N has been observed, well before maximum light. The premaximum spectra (Leibundgut et al. 1991a) have revealed the following new features of a SN Ia: (1) The rise time to maximum brightness is as long as $\sim 20$ days. (2) The expansion velocities of Si and Ca are higher than previously measured in SNe Ia, extending to $v_{\rm exp} \sim 20{,}000$ km s$^{-1}$. (3) The Fe and Co lines are present in the spectrum two weeks before the maximum.

Leibundgut et al. (1991a) have mentioned that the above new features (2) and (3) are difficult to account for with the carbon deflagration model, since the highest velocities of newly synthesized Si and Ca are $\sim 15{,}000$ km s$^{-1}$ in the carbon deflagration model W7.

We first would like to point out that the newly observed features of SN 1990N can be explained with model W7, if the heavy elements synthesized by a deflagration in the inner layers are mixed to the high-velocity outer layers (Possibility I). Branch et al. (1985) and Branch & Venkatakrishna (1986) invoked such a mixing to account for the observed spectra. This possibility is still an open question, since Harkness (1991) obtained an excellent agreement between the calculated and observed spectra of SN 1989B without mixing.

Another possible model being a slightly modified version of W7 is that the high-velocity heavy elements are produced by a detonation that is ignited in the outermost layers. Nomoto et al. (1984) noted that the carbon deflagration of case C8, whose propagation speed is slightly higher than W7, induces a detonation in the outer layers (see also Woosley & Weaver 1986a). Since nucleosynthesis in the outer detonation (e.g., Si/Ni ratio) depends sensitively on the density at the transformation from the deflagration to the detonation, some cases may account for the observed features of SN 1990N; in this case, the premaximum Si/Ca are the products of the detonation while the features near maximum light and later phase are due to the deflagration (Possibility II; Yamaoka et al. 1992).

The model which may account for the entire spectral features by the products of detonation may also be possible (Possibility III). This delayed detonation model (Khokhlov 1991a,b; Woosley & Weaver 1991) starts from a very slow deflagration and assumes its transformation into a detonation relatively deep inside the star. Afterwards the detonation produces both iron peak elements and intermediate mass elements. Note, however, that the initially slow deflagration model has stronger constraints than W7 on the initial central density and metallicity of the white dwarf to avoid overproduction of some neutron-rich elements (Khokhlov 1991b; Woosley & Weaver 1991).

In the present *Letter*, we propose another possible carbon detonation model that could form in white dwarfs with masses $\sim 1.0\ M_\odot$ (Possibility IV). The possible evolutionary origin is discussed in § 2. Because of the low initial central densities, the nucleosynthesis of the carbon detonation is able to account for the observed features of SN Ia 1990N (§ 3).

We also demonstrate that the slow rise of the light curve of SN 1990N can be reproduced well by both the deflagration

and detonation models if the optical opacity is somewhat larger than previously adopted. New estimates of the Hubble constant from the slow rise models of Type Ia SNe are given in § 4.

## 2. EVOLUTIONARY SCENARIO

In the standard scenario of accreting white dwarf models for SNe Ia, the white dwarf grows in mass toward the Chandrasekhar mass and ignites explosive carbon burning at a central density as high as $\sim 3 \times 10^9$ g cm$^{-3}$ (e.g., Nomoto 1982a, 1986).

It might be the case that some fraction of SNe Ia originate from different types of presupernova evolution. In particular, an explosive carbon ignition could occur in C + O white dwarfs whose masses are significantly smaller than the Chandrasekhar mass. Such a possibility has been discussed in the context of the merging double white dwarf scenario (Iben & Tutukov 1984; Webbink 1984). During merging, an off-center carbon flash is likely to be ignited in the more massive white dwarf as a result of (1) compressional heating due to rapid accretion (Nomoto & Iben 1985), (2) dynamical compression due to merging (Iben 1988; Wheeler & Harkness 1990), or (3) the formation of a thick disk around the white dwarf (Benz et al. 1990) and the subsequent heat generation at the boundary layer (Mochkovitch & Livio 1990).

The strength of the carbon flash is sensitive to the density at the ignited shell. The rapid accretion in the previous spherical models ignites carbon at $\sim 1$–$3 \times 10^6$ g cm$^{-3}$, which does not directly lead to the formation of a shock wave (Nomoto & Iben 1985; Saio & Nomoto 1985). However, if the ignition density would be a little higher in the nonspherical accretion or convective energy transport during the carbon flash is much less efficient than in the above spherical models, the flash could lead to a thermonuclear runaway and form shock waves (not a detonation) that propagate both inward and outward.

The inward shock wave, once formed, could propagate toward the central region and increase its strength because of a decreasing surface area at the shock front (e.g., Ono 1960). For the case of off-center helium detonation, Livne (1990) found that the resulting inward shock wave is strong enough to detonate carbon at the center with $\rho_c \gtrsim 10^7$ g cm$^{-3}$. Successive off-center carbon flashes may have a similar cumulative effect to form a shock wave that is strong enough to initiate a carbon detonation.

This scenario, though highly hypothetical yet, could lead to the formation of a carbon detonation wave in the white dwarfs of masses as small as $\sim 1.0\ M_\odot$. The mass of the white dwarf before merging is likely to be around $1.0\ M_\odot$ if it is formed from case BB binary evolution; in this case, a star with an initial mass of 5–8 $M_\odot$ becomes a helium star of 1.5–2 $M_\odot$, which greatly expands to undergo Roche lobe overflow when its degenerate C + O core grows to $\sim 1\ M_\odot$ (e.g., Rose 1969; Sugimoto 1971; Paczyński 1971; Sugimoto & Nomoto 1980; Nomoto 1982b).

## 3. CARBON DETONATION IN SMALL MASS WHITE DWARFS

Hydrodynamical calculations are performed for bare hydrostatic white dwarfs of masses $M = 1.0$–$1.2\ M_\odot$. The central densities for $M = 1.03$, 1.05, and $1.07\ M_\odot$ are 2.5, 3, and $4 \times 10^7$ g cm$^{-3}$, respectively. The initial composition is set that the mass fractions of $^{12}$C, $^{16}$O, and $^{22}$Ne are 0.48, 0.50, and 0.02. This corresponds to the Population I composition where $^{14}$N is processed into $^{22}$Ne yielding a neutron excess of 0.002 ($Y_e = 0.499$).

The numerical calculation is performed with a one-dimensional Lagrangian PPM code (Colella & Woodward 1984; Colella & Glaz 1985). Hydrodynamical equations are solved simultaneously with a nuclear reaction network consisting of 13 species (Müller 1986) with added $(\alpha, p)(p, \gamma)$ channels to the $(\alpha, \gamma)$ reaction. After hydrodynamical calculations are made, the detailed nucleosynthesis is calculated with a larger nuclear reaction network of 299 species (Thielemann, Nomoto, & Yokoi 1986; Thielemann, Hashimoto, & Nomoto 1990). The remaining input physics are basically the same as adopted in Nomoto & Kondo (1991).

In our calculations, the detonation is initiated by artificially igniting a carbon flash at the center and enhancing the heat conduction across the burning front to speed up the propagation of a deflagration wave. The detonation wave quickly develops to propagate self-consistently at the speed of a Chapman-Jouguet detonation. Behind the detonation wave, material undergoes explosive burning of silicon, oxygen, neon, and carbon, depending on the peak temperatures $T_p$, which depend mainly on the initial densities of the material, $\rho_0$. The composition structure of the detonated white dwarf of $M = 1.03\ M_\odot$ (model CDT3) after reaching the homologous expansion stage is shown as a function of $v_{\rm exp}$, $\rho_0$, and $M_r$ in Figure 1.

In the inner layers at $\rho_0 \gtrsim 1 \times 10^7$ g cm$^{-3}$, $T_p \gtrsim 5.3 \times 10^9$ K so that nuclear reactions are rapid enough to incinerate the material into mostly $^{56}$Ni. This density range corresponds to the α-rich freeze-out, so that some He and $^{58}$Ni [via $^{54}$Fe $(\alpha, \gamma)$] are produced as well. In the outer layers of lower densities, $^{56}$Ni and $^{54}$Fe are produced from incomplete silicon burning and Ca, Ar, S, and Si are produced from explosive oxygen burning. Trace $^{56}$Ni is produced until $\rho_0$ becomes lower than $\sim 2.5 \times 10^6$ g cm$^{-3}$. At $\rho_0 \lesssim 2.5 \times 10^6$ g cm$^{-3}$, oxygen

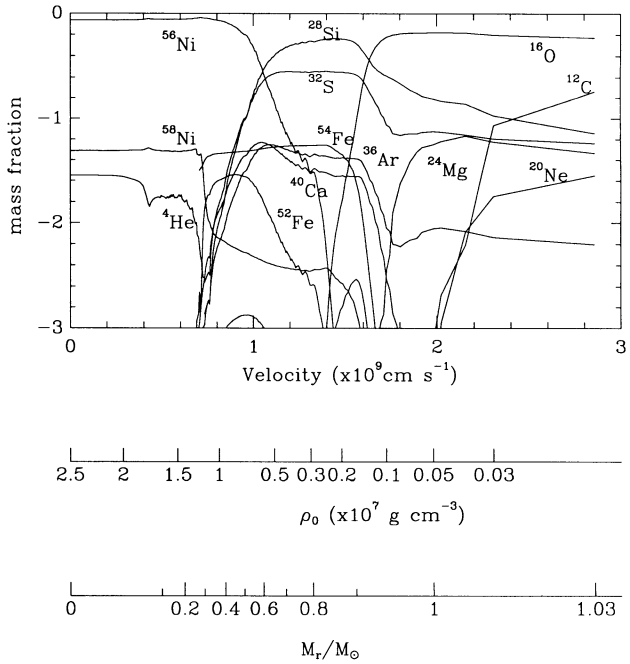


FIG. 1.—Composition of the carbon model CDT3 (a $1.03\ M_\odot$ white dwarf) as function of the expansion velocity, $M_r$, and the initial density $\rho_0$.

burning becomes incomplete but still produces significant amounts of Ca, Ar, S, and Si. In the outermost layers with $\rho_0 \lesssim 1 \times 10^6$ g cm$^{-3}$, explosive burning of carbon and neon synthesizes Ar, S, Si, and Mg with some unburned O and C.

Model CDT3 produces a $^{56}$Ni mass of $M_{Ni} = 0.49\ M_\odot$ and an explosion energy $E = 1.2 \times 10^{51}$ ergs s$^{-1}$. For a white dwarf with a larger mass $M$ and thus a higher central density, more $^{56}$Ni is produced and a larger explosion energy $E$ is generated. For $M = 1.05\ M_\odot$ (CDT5) and $1.07\ M_\odot$ (CDT7), $M_{Ni} = 0.56$ and $0.67\ M_\odot$, and $E = 1.3$ and $1.4 \times 10^{51}$ ergs, respectively. For $M > 1.2\ M_\odot$, the Si-rich layer would be too thin in mass to be compatible with the SN Ia spectra.

Other important nucleosynthesis features found from Figure 1 are as follows:

(1) Because of low central densities, neutronization due to electron capture is negligible. The production of neutron-rich iron-peak elements, $^{62}$Ni, $^{58}$Ni, and $^{54}$Fe, is due entirely to the preexistence of $^{22}$Ne. Therefore $^{56}$Ni is dominant in the central region, unlike the dominance of neutron-rich iron peak elements in the central region of the carbon deflagration model.

(2) The low-density layers of incomplete silicon and oxygen burning extend much wider in mass, starting at $M_r = 0.3\ M_\odot$. Thus the composition structure of the Si-rich outer layers is similar to that of W7. Differing from W7, however, the Si and Ca layers extend to expansion velocities higher than 15,000 km s$^{-1}$, ranging from 7500 to 28,000 km s$^{-1}$ for Si and 7500–18,000 km s$^{-1}$ for Ca. For CDT5 and CDT7, the minimum velocity of Ca/Si is $\sim$8500 and 9500 km s$^{-1}$, respectively. These composition structures in velocity space would be favorable to account for the spectra of SN 1990N.

The isotopic ratios of integrated abundances of ejecta after decay of unstable nuclei with respect to solar abundances are given in Nomoto et al. (1991). Because of the low neutron excess, overproductions of $^{54}$Fe and $^{58}$Ni, are not observed even with the Population I metallicity and the isotopic ratios of iron peak elements are within a factor of 2 relative to their solar ratios. This is an important difference from the carbon deflagration/detonation models with $M \sim 1.4\ M_\odot$.

## 4. LIGHT CURVES AND THE HUBBLE CONSTANT

Light curves of the detonated white dwarfs are powered by the radioactive decay chain $^{56}\text{Ni} \rightarrow {}^{56}\text{Co} \rightarrow {}^{56}\text{Fe}$. The original $\gamma$-ray energy is partly lost as $\gamma$-ray emissions and partly deposited in the ejecta through multiple Compton scatterings and atomic processes. In the present study, the rate of $\gamma$-ray energy deposition is obtained by calculating the $\gamma$-ray absorption opacity, which is 0.03 cm$^2$ g$^{-1}$ (Shigeyama & Nomoto 1990; Sutherland & Wheeler 1984). The calculated energy deposition rates for the model CDT3 ($M = 1.03\ M_\odot$) and W7 are shown by the dashed lines in Figures 2 and 3, respectively, which are in good agreement with Monte Carlo simulations of the $\gamma$-ray transport (Kumagai et al. 1989; Ambwani & Sutherland 1988).

For the optical light curve, radiative transfer is calculated with the flux-limited diffusion approximation (Shigeyama & Nomoto 1990). We assume a constant optical opacity of $\kappa = 0.1$, 0.2, and 0.3 (in units of cm$^2$ g$^{-1}$ hereafter) to examine the dependence of the light curve shape on $\kappa$.

The calculated bolometric light curves for CDT3 are shown by the solid curves in Figure 2 for the three cases of optical opacity. Maximum brightness is reached when the expansion time scale becomes comparable to that of heat diffusion from the radioactive source. The light curve shape thus depends on

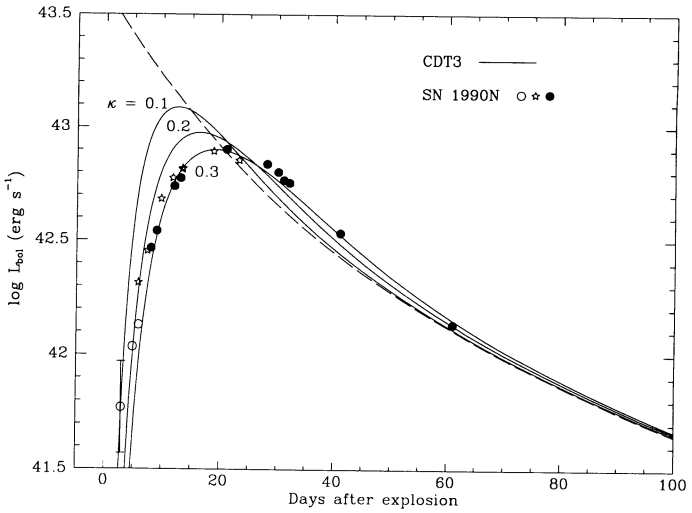


FIG. 2.—Calculated bolometric light curves of the carbon detonation model CDT3 for $\kappa = 0.1$, 0.2, and 0.3 cm$^2$ g$^{-1}$ (*solid lines*) are compared with the observed visual light curve of SN 1990N. The open circles show the OCA (IAU Circ. 1990, No. 5039) and Asiago (IAU Circ. 1990, No. 5039, 5040) observations, and the star marks and filled circles are, respectively, the *IUE* FES and CTIO observations (Leibundgut et al. 1991a).

the effective diffusion time $(\kappa M/v_{exp}\ c)^{1/2}$ (Arnett 1982). Therefore the date of the maximum $t_{max}$ is earlier and thus the maximum luminosity $L_{max}$ is higher for smaller $\kappa$ and higher $v_{exp}$. For $\kappa = 0.1$, 0.2, and 0.3, $t_{max} = 12$, 16, and 19 days and $L_{max} = 1.2$, 0.93, and $0.79 \times 10^{43}$ ergs s$^{-1}$, respectively. After the peak, the bolometric luminosity gets closer to the energy deposition rate.

The bolometric light curves of the carbon deflagration model W7 are shown in Figure 3 also for three cases of $\kappa$. Compared with CDT3, $L_{max}$ is higher because of a larger $^{56}$Ni mass, and the decline is slightly slower because of smaller $E/M$ ($M = 1.38\ M_\odot$, $M_{Ni} = 0.58\ M_\odot$, $E = 1.3 \times 10^{51}$ ergs s$^{-1}$). However, the decline of W7 is not so different from CDT3 because $^{56}$Ni is distributed at $M_r \approx 0.2$–$0.8\ M_\odot$, not confined to the central region (Graham 1987; Nomoto & Shigeyama 1991).

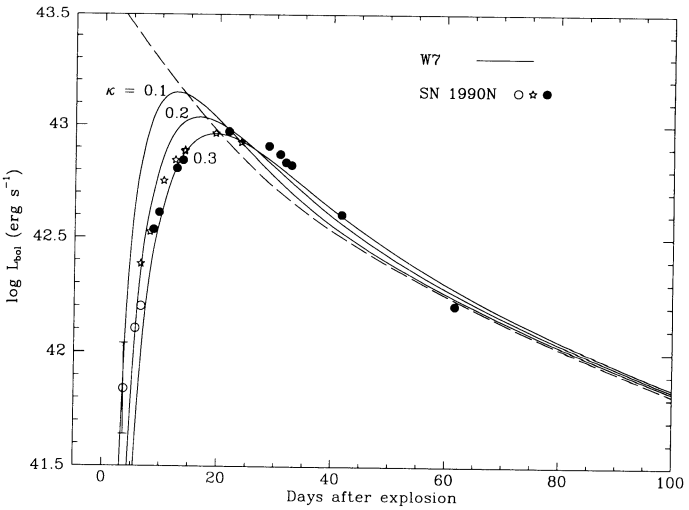


FIG. 3.—Same as Fig. 2 but for the carbon deflagration model W7

The observed visual light curve of SN 1990N is shown in Figures 2 and 3 (see Leibundgut et al. 1991a, and figure captions). The maximum brightness of SN 1990N is arbitrarily shifted to the calculated $L_{max}$. It is seen that the light curves of CDT3 and W7 with $\kappa = 0.3$ are both in reasonable agreement with SN 1990N. Since the bolometric light curve is regarded to be close to the visual one, this agreement is encouraging for a further study, whether the explosion model has actually an expansion opacity as large as $\kappa = 0.3$ on the average (Karp et al. 1977; Harkness 1991; Höflich, Khokhlov, & Müller 1991; Khokhlov, Müller, & Höflich 1991).

The maximum brightness $L_{max}$ of SNe Ia when explained with radioactive decay models has been used to estimate the Hubble constant $H_0$ (in units of km $s^{-1}$ $Mpc^{-1}$ hereafter). From the well-observed six SNe Ia, Arnett, Branch, & Wheeler (1985) derived $L_{max} \sim 1.9 \pm 0.3 \times 10^{43} (H_0/50)^{-2}$ ergs $s^{-1}$.

The maximum brightness of radioactive decay models depends on the date of maximum light $t_{max}$. For W7, $L_{max} =$ 1.4, 1.1, and $0.92 \times 10^{43}$ ergs $s^{-1}$ at $t_{max} = 13$, 16, and 20 days ($\kappa = 0.1$, 0.2, and 0.3), which gives $H_0$ ($\pm 6$) = 58, 66, and 72, respectively. Model CDT3 has a smaller $M_{Ni}$ (0.49 $M_\odot$), so that the corresponding $\kappa$-values give $H_0$ ($\pm 6$) = 63, 71, and 77, respectively.

The mass of $^{56}$Ni may be constrained from the minimum expansion velocities of Ca and Si, which is estimated to be $\sim$8000 km $s^{-1}$ for SN 1981B (Branch et al. 1983; Harkness 1991). This velocity in model CDT3 is $\sim$7500 km $s^{-1}$, so that $M_{Ni} \sim 0.5\ M_\odot$ would be the minimum among the carbon detonation models.

If $t_{max} \sim 20$ days would be common for most SNe Ia, $H_0 \sim$ 60–83 is inferred from the models with $M_{Ni} = 0.49$–$0.67\ M_\odot$ considered here. For larger $M$ models with larger $M_{Ni}$, $H_0$ may be roughly scaled as $M_{Ni}^{1/2}$. Note, however, that the above estimate of $H_0$ is subject to uncertainties involved in (1) the expansion opacity and (2) the determination of $M_{Ni}$.

## 5. DISCUSSION

To discriminate between the four possible explanations of the observed features of SN 1990N (Possibilities I–IV in § 1), further detailed studies are necessary. Observationally it needs to be clarified, whether or not a slow rise light curve like SN 1990N is common for SNe Ia (or forms a distinct subclass); note that the recently corrected premaximum light curve of SN 1981B (Leibundgut 1991) shows a significantly slower rise than previously reported (Leibundgut et al. 1991b).

The carbon detonation models in low mass white dwarfs can account for the basic features of SNe Ia with a restricted range of white dwarf mass ($M \approx 1.0$–$1.2\ M_\odot$). Variation of $M$ naturally yields the observed variation of the expansion velocity of Si (e.g., Branch, Drucker, & Jeffery 1988; Benetti, Cappellaro, & Turatto 1991). This mass range might be preferentially realized for the 5–8 $M_\odot$ progenitors through the case BB close binary evolution to form double degenerates (§ 2).

Therefore, much work needs to be done for the still highly hypothetical scenario of presupernova evolution. This includes: (1) hydrodynamics of the merging process of double white dwarfs, (2) determination of the off-center carbon ignition conditions, (3) effects of outward and inward shock waves on the pre-detonation white dwarf density structure, and (4) possible effects of a thick disk around the detonating white dwarf.

We would like to thank D. Branch, P. Höflich, D. Jeffery, A. Khokhlov, B. Leibundgut, and E. Müller for stimulating discussions. T. S. thanks E. Müller for providing the network solver. This work has been supported in part by the Ministry of Education, Science, and Culture in Japan (grants 02302024 and 03218202) and NSF grant AST-8913799. Part of the calculations were performed at the NCSA (AST 890009N).

## REFERENCES

Ambwani, K., & Sutherland, P. 1988, ApJ, 325, 820
Arnett, W. D. 1982, ApJ, 253, 785
Arnett, W. D., Branch, D., & Wheeler, J. C. 1985, Nature, 314, 337
Benetti, S., Cappellaro, E., & Turatto, M. 1991, A&A, 247, 410
Benz, W., Bowers, R. L., Cameron, A. G. W., & Press, W. 1990, ApJ, 348, 647
Branch, D., Doggett, J. B., Nomoto, K., & Thielemann, F.-K. 1985, ApJ, 294, 619
Branch, D., Drucker, W., & Jeffery, D. 1988, ApJ, 330, L117
Branch, D., Lacy, C. H., McCall, M. L., Sutherland, P. G., Uomoto, A., Wheeler, J. C., & Wills, B. J. 1983, ApJ, 270, 123
Branch, D., Nomoto, K., & Filippenko, A. V. 1991, Comm. Astrophys., XV, 221
Branch, D., & Venkatakrishna, K. L. 1986, ApJ, 306, L21
Colella, P., & Glaz, H. M. 1985, J. Comput. Phys., 59, 264
Colella, P., & Woodward, P. R. 1984, J. Comput. Phys., 54, 174
Graham, J. R. 1987, ApJ, 315, 588
Harkness, R. P. 1991, in SN 1987A and Other Supernovae, ed. I. J. Danziger (Garching: ESO), 447
Höflich, P., Khokhlov, A. M., & Müller, E. 1991, A&A, 248, L7
Iben, I., Jr. 1988, ApJ, 324, 355
Iben, I., Jr., & Tutukov, A. 1984, ApJS, 55, 335
Karp, A. H., Lasher, G., Chan, K. L., & Salpeter, E. E. 1977, ApJ, 214, 161
Khokhlov, A. M. 1991a, A&A, 245, 114
———. 1991b, A&A, 245, L25
Khokhlov, A. M., Müller, E., & Höflich, P. 1991, A&A, submitted
Kumagai, S., Shigeyama, T., Nomoto, K., Itoh, M., Nishimura, J., & Tsuruta, S. 1989, ApJ, 345, 412
Leibundgut, B. 1991, private communication
Leibundgut, B., Kirshner, R. P., Filippenko, A. V., Shields, J. C., Foltz, C. B., Phillips, M. M., & Sonneborn, G. 1991a, ApJ, 371, L23
Leibundgut, B., Tammann, G. A., Cadonau, R., & Cerrito, D. 1991b, A&AA, 89, 537
Livne, E. 1990, ApJ, 354, L53
Mochkovitch, R., & Livio, M. 1990, A&A, 236, 378
Müller, E. 1986, A&A, 162, 103
Nomoto, K. 1982a, ApJ, 253, 798
———. 1982b, in Supernovae: A Survey of Current Research, ed. M. J. Rees and R. J. Stoneham (Dordrecht: Reidel), 210
———. 1986, Ann. NY Acad. Sci., 470, 294
Nomoto, K., & Iben, I., Jr. 1985, ApJ, 297, 531
Nomoto, K., & Kondo, Y. 1991, ApJ, 367, L19
Nomoto, K., & Shigeyama, T. 1991, in Supernovae, ed. S. E. Woosley (Berlin: Springer), 572
Nomoto, K., Sugimoto, D., & Neo, S. 1976, ApSS, 39, L37
Nomoto, K., Thielemann, F.-K., & Yokoi, K. 1984, ApJ, 286, 644
Nomoto, K., Yamaoka, H., Shigeyama, T., Kumagai, S., & Tsujimoto, T. 1991, in Supernovae (Les Houches, Session LIV), ed. J. Audouze et al. (New York: Elsevier), in press
Ono, Y. 1960, Prog. Theor. Phys., 24, 825
Paczyński, B. 1971, Acta Astron., 21, 1
Rose, W. K. 1969, ApJ, 155, 491
Saio, H., & Nomoto, K. 1985, A&A, 150, L21
Shigeyama, T., & Nomoto, K. 1990, ApJ, 360, 242
Sugimoto, D. 1971, Prog. Theor. Phys., 45, 761
Sugimoto, D., & Nomoto, K. 1980, Space Sci. Rev., 25, 155
Sutherland, P., & Wheeler, J. C. 1984, ApJ, 280, 282
Thielemann, F.-K., Hashimoto, M., & Nomoto, K. 1990, ApJ, 349, 222
Thielemann, F.-K., Nomoto, K., & Yokoi, K. 1986, A&A, 158, 17
Webbink, R. 1984, ApJ, 277, 355
Wheeler, J. C., & Harkness, R. 1990, Rep. Progr. Phys., 53, 1467
Woosley, S. E., & Weaver, T. A. 1986a, Lecture Notes in Physics, 255, 91
———. 1986b, ARA&A, 24, 205
———. 1991, in Supernovae (Les Houches, Session LIV), ed. J. Audouze et al. (New York: Elsevier), in press
Yamaoka, H., Nomoto, K., Shigeyama, T., & Thielemann, F.-K. 1992, in preparation